Chapter 6
Cu-Fe prussian blue analog nanocube with intrinsic oxidase mimetic behaviour for the non-invasive colorimetric detection of Isoniazid in human urine.

6.1 Introduction

Owing to very high efficacy and hypo toxicity, Isoniazid (INH) is a crucial first-line antibiotic against a severe and infectious respiratory disease named Tuberculosis [Xiong et al., 2007; Fernandes et al., 2017]. However, any discrepancy in the INH concentration in the blood may lead to liver impairment, neural toxicity, and drug resistance. The therapeutic window for the INH in the treatment of Tuberculosis is 3-6 μg/mL in serum, and the median concentration in plasma is 2.6 μg/mL (range 0.5 to 12.1 μg/mL), which is typically achieved by taking a dose of 300 mg for the patient with weight > 50 Kg [Park et al., 2016; Lempens et al., 2018; Prahl et al., 2014]. Therefore, it becomes compulsory to design a comfortable and sensitive methodology that can monitor the INH concentration in the human body. There are many reports available for the quantification of the INH that includes High-performance Liquid Chromatography (HPLC) [Bhandari et al., 2012], electrochemistry [Rastogi et al., 2016; Jena et al., 2010], gas chromatography [Khuhawar et al., 2006], fluorescence spectrophotometry [Wang et al., 2018; Ma et al., 2021]. Even though these methods have good significance, they require sophisticated instrumentation and skilled labor with multistep sampling making them expensive and incompetent for practical applications. The colorimetric method provides an alternative to these limitations. It provides easy, rapid, and naked-eye detection of the analyte in the real sample, with significant progress in the last decades [He et al., 2020]. Recently nanomaterials with enzyme-like characteristics (nanozymes) have drawn much attention in colorimetric assay over natural enzymes like Horseradish peroxidase (HRP) as natural enzymes with

shallow stability, low recyclability due to denaturation, and expensive isolation methods [Veitch et al., 2004; Xianyu et al., 2013]. Oxidase mimics bear an advantage over other enzyme mimics and catalyze the oxidation of the chromogenic substrates without any requirement of corrosive H_2O_2, making them competent for developing user-friendly sensors having better constancy [He et al., 2020]. In this regard, many nanostructures with enzymatic behaviour have been uncovered for e.g. gold nanoparticles (AuNPs) [Vinita et al., 2018], silver nanoparticles (AgNPs) [Ojha et al., 2020], platinum nanoparticles (PtNPs) [Kora et al., 2018], Au-Pd bimetallic nanocomposite [Singh et al., 2017]. Noble metals have very high costs, and they are prone to aggregation, limiting their long-term storage and use, and deterring them from practical applications. Inorganic transition metals-based enzyme mimics have drawn great attention for the development of cost-effective and stable colorimetric devices, as they are cheap, easy to synthesize, and have better stability and tunable catalytic activity, e.g., Fe_3O_4 magnetic nanoparticles (MNPs) [Wei et al., 2008], Molybdenum disulfide nanosheet (MoS_2) [Nirala et al., 2018], Vanadium pentoxide nanowire (V_2O_5) [Andre et al., 2011], Manganese dioxide (Mn_3O_4) [Zhang et al., 2015], etc. Among them, Prussian blue analogues (PBAs) are an important class of metal-organic frameworks (MOFs) with the formula of $A_xM_y[M'(CN)_6]$. zH_2O (where M and M′ represent transition metal elements and A denotes an alkali metal ion). PBAs have found extensive application in the area of oxygen reduction, hydrogen evolution, energy storage, and biosensing owing to its high specific surface areas and excellent electron-transport properties. The structural framework of PBAs is comprised of octahedral MN_6 and $M'C_6$ and units linked together by cyanide ligands, where octahedral sites are occupied alternately by M and M′ metals and ordered through co-ordination bonds linking with respective nitrogen and carbon [Li et al., 2020]. Due to their low cost, high stability, tunable size, and good

electrocatalytic properties, nanosized PBAs have been extensively applied as a platform for the sensing of dopamine [Karikalan et al., 2016], carcinoembryonic antigen [He et al., 2019], methyl parathion [Li et al., 2014], guanine [Li et al., 2020], etc. Recently, PBAs have been exclusively focused on as they possess excellent enzyme mimetic behavior with wide potential in the field of colorimetric assay [Chen et al., 2018; Wang et al., 2020].

In the present study, we have synthesized Cu-Fe Prussian blue analog nanocube (CuFe-PBA-NC) using a simple precipitation method. The synthesized CuFe-PBA-NC has intrinsic oxidase mimetic activity for TMB substrate with dissolved O_2. The CuFe-PBA-NC nanonzyme kinetic study validates their high affinity toward chromogenic substrate TMB with remarkably high enzyme velocity. These properties have prompted us to develop a colorimetric sensor for an anti-tuberculosis drug (INH). The INH has a pyridine ring with a strong reductive hydrazyl group, which may lead to competitive inhibition of the oxidase behavior of the nanocube with TMB [He et al., 2020]. The INH introduction in CuFe-PBA-NC catalyzed TMB oxidation consequences to a colorless product with inefficient enzyme catalysis. We have developed a colorimetric strategy to quantify the INH in human urine based on this inhibition concept. We have also developed a portable kit for onsite detection of the INH in the real sample (urine). We hope the proposed method will be very much helpful in the treatment and monitoring of tuberculosis disease.

6.2 Experimental

6.2.1 Materials and Instrumentation

Copper chloride dihydrate, Sodium Citrate, Potassium ferricyanide, sodium acetate, acetic acid, Isoniazid (INH) and 3,3’,5,5’-tetramethylbenzidine (TMB), Creatinine (Creat), Magnesium oxide, sodium chloride, potassium chloride, glucose (Glu), urea,

uric acid (UA) were purchased from Sigma Aldrich. Deionized water (DI) (dI (pH=7, resistivity=18.0 MΩ) was taken for the solution preparation in all experiments. Rigaku miniflex 600 X-ray diffractometer with Cu Kα1 radiation (λ = 1.54056 Å was used for X-ray powder diffraction measurement of the prepared CuFe-PBA-NC. The surface property of the material was investigated from Nova Nano SEM-450, FEI, USA and NTEGRA Prima, NT-MDT scanning probe microscope. UV-visible absorption spectra of the material were recorded with a Biotek spectrophotometer (Epoch 2, USA), and FT-IR analysis was carried out in the spectral range of 450-4000 cm^{-1} with a Thermo Scientific Nicolet 6700 FTIR spectrometer. The chemical environment of the elements present in the material was by Thermoscientific K-Alpha X-ray photoelectron spectrometer. The surface area and pore size of the sample was analyzed on BET surface area analyzer (BEL Japan) With the help of N_2 adsorption/desorption isotherms at 77 K. The urine sample has been collected voluntarily from the healthy person for testing.

6.2.2 Synthesis of the CuFe-PBA-NC

To synthesize CuFe-PBA-NC, 0.6 mmol of copper chloride dihydrate and 0.9 mmol of sodium citrate were added to 20 mL of DI water, then 20 mL of an aqueous solution of 0.4 mmol potassium ferricyanide was added dropwise in this solution at stirring condition (460 rpm). After addition, stirring was maintained for 20 minutes to prepare a homogenous mixture. The resultant reaction mixture was aged for two days without disturbing it at room temperature (RT).

6.2.3 Study of Oxidase activity of CuFe-PBA-NC

To investigate the oxidase behavior of CuFe-PBA-NC aqueous medium, we have recorded the absorption spectrum in different combinations. The selected combinations include (a) x+y+z (b) x+y+z+r (c) x+y, where x is 100 µL of acetate buffer (0.1 M;

pH=4.0), y is 100 µL of TMB (400 µM), z is 10 µL of CuFe-PBA-NC (1 mg/mL), and r denotes INH (100 µL; 40 µM).

6.2.4 Colorimetric assay of INH

The oxidase property of the nanozymes has been further exploited for the colorimetric sensing of INH detection. In a particular experiment, 100 µL of 0.1 M acetate buffer of pH=4.0, INH (1µM to 100 µM) and CuFe- PBA-NC (10 µL; 1mg/mL) solutions were added to an 0.5 mL Eppendorf. Further, 100 µL of 400 µM TMB was added. The reaction mixture was transferred into a 96-well ELISA plate after incubating it for 20 mins at RT for recording endpoint (λ_{max} =652 nm) and absorption spectrum.

6.2.5 Interference study

The interferences from the urine components have been investigated, keeping their concentration ten-fold greater than the INH. CuFe-PBA-NC (10 µL) solution, acetate buffer (0.1M, 100 µL) and 100 µL of the TMB solution (400 µM) has been added to all the samples and incubated for the 20 mins at room temperature. The reaction mixture was further added to ELISA wells, and the endpoint was recorded at λ_{max}=652 nm.

6.3 Results and Discussion

6.3.1 Materials Characterization

The structural investigation of the synthesized CuFe-PBA-NC has been performed using Fourier transform infrared (FTIR) spectroscopy. Figure 6.1(a) shows the FTIR spectrum in which the peak positioned at lower wavenumber, 1603 cm^{-1} assigned for H-O-H bending mode and at higher wavenumber, 3441 cm^{-1} due to O-H stretching mode, demonstrating the existence of water molecules in the framework. The bands at 2094 cm^{-1} and 2172 cm^{-1} are related to Cu(II)-N≡C-Fe(II) and Cu(II)-N≡C-Fe(III) species, respectively, signifying the nature of the C≡N bond existing in the molecule [Ojwang et

al., 2016; Cheng et al., 2019]. The FTIR spectrum gives the idea of the functional units present in the PBA. The crystal structure of the synthesized CuFe-PBA-NC was investigated by the X-ray diffraction technique (XRD). The peaks at 15.12, 17.37, 24.71, 29.21, 35.27, 39.67, 43.77, 50.81, 54.33, 57.27, 66.36, 69.29 can be attributed to (111), (200), (220), (311), (400), (420), (422), (440), (600), (620), (640), (642) planes respectively. As shown in Figure 6.1 (b), the observed peaks have been compared and found to be well consistent with standard JCPDS file no. 70-2702. The XRD peaks validate the synthesis of prussian blue analog according to previous reports [Xing et al., 2020; Xie et al., 2019].

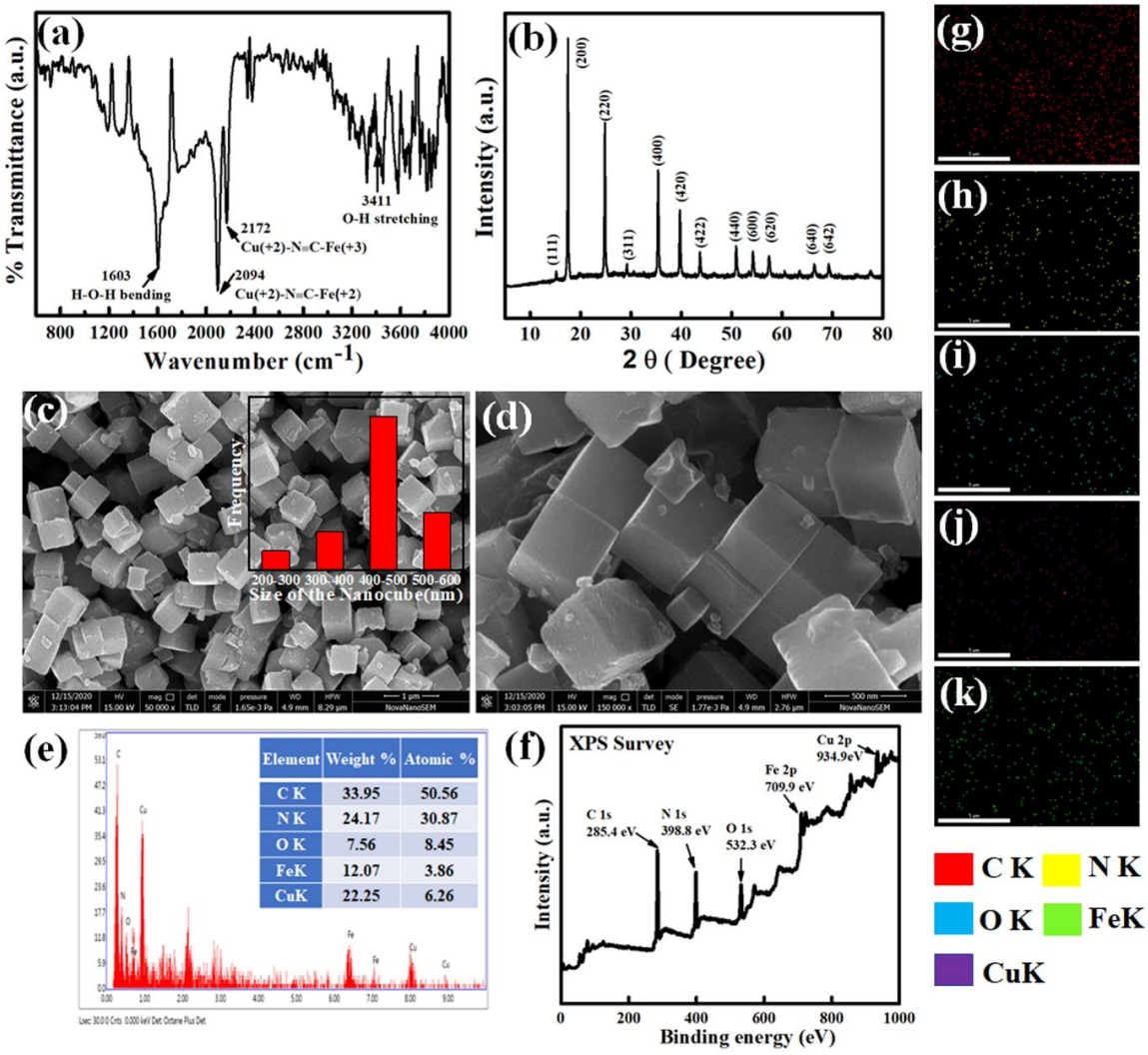

Figure 6.1. (a) FTIR spectrum of CuFe-PBA-NC, (b) XRD spectrum (c) SEM image at 1 μm scale, (inset c) size distribution histogram, (d) SEM image at 500 nm scale, (e) EDS spectrum, (f) XPS survey, (g) Elemental mapping image of C, (h) N, (i) O, (j) Fe, and (k) Cu.

The morphological studies have been done using SEM. The SEM image (Figure 6.1 (c &d)) shows the nanocube structure of the synthesized CuFe-PBA-NC having a maximum frequency in the range of 400-500 nm, as can be seen in the size distribution histogram (Inset Figure 6.1 c). Figure 6.1 (e) shows the energy dispersive X-ray (EDX) used for further investigation of the elemental compositions of the CuFe-PBA-NC synthesized. One can observe that C, N, O, Fe, and Cu are present in synthesized CuFe-PBA-NC validating its successful synthesis. Also, the EDS mapping image (Figure 6.1

(g-k)) corresponds to the different elements, validates the composition and distribution in the nanocube, and supports our synthesis.

For further confirmation of the structure, XPS of the CuFe-PBA-NC was performed. Figure 6.1 (f) shows the XPS survey spectrum having the peaks corresponding to Fe, Cu, N, C, and O elements confirming its elemental composition. Deconvoluted high-resolution spectra of all the elements are shown in Figure 6.2. In the high-resolution spectrum of Cu 2p, peaks located at 932.8 ($2p_{3/2}$) and 951.2 ($2p_{1/2}$) eV can be allocated for Cu(0), and peaks fitted at 935.5, and 952.6 eV belongs to Cu^{2+} species shown in Figure 6.2 (a). The satellite peaks at around 942.6 and 944.5 eV reconfirm the presence of Cu^{2+} [Xie et al., 2019; Cheng et al., 2020]. In the spectrum of Fe 2p (Figure 6.2 (b)), peaks at lower binding energies 708.9 (Fe $2p_{3/2}$) and 721.2 (Fe $2p_{1/2}$) eV corresponds to Fe^{2+} and peaks observed at higher binding energies 711.5 (Fe $2p_{3/2}$) and 723.6 (Fe $2p_{1/2}$) eV due to the presence of Fe^{3+} in CuFe-PBA-NC, which introduces two spin-orbit doublets in the material [Xing et al., 2020]. The mixed-valence state of two metals Cu and Fe atoms, present in the structure may enhance the oxidase catalytic property by increasing the electron transfer rate [Xuan et al., 2017].

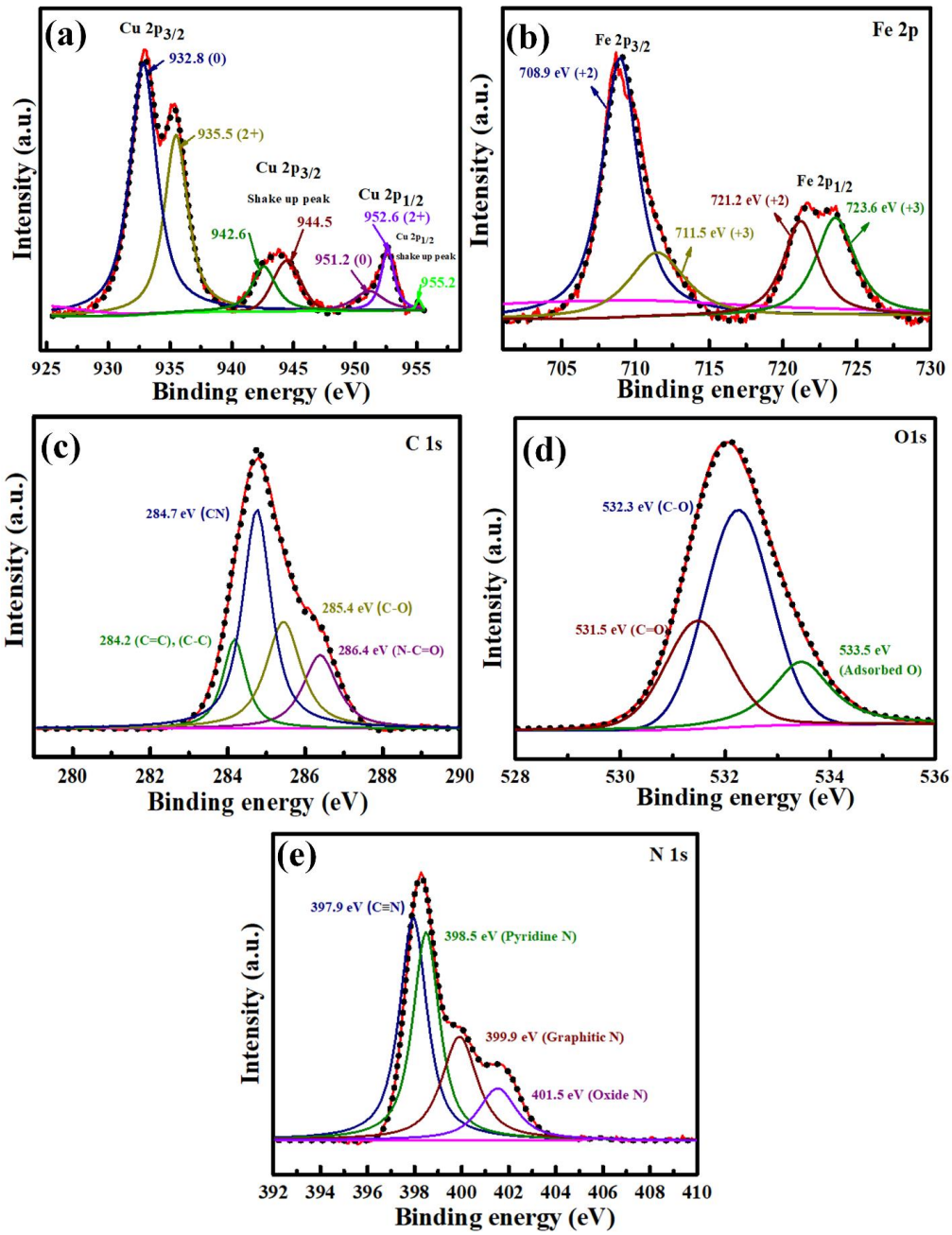

Figure 6.2. Deconvoluted XPS spectrum corresponding to (a) Cu, (b) Fe, (c) C, (d) O, and (e) N.

The high-resolution spectrum of C1s is shown in Figure 6.2(c), in which the characteristic peak of C≡N appears at 284.7 eV while other peaks at binding energies 284.2, 285.4, and 286.4 eV correspond to C=C (C-C), C-O, and N-C=O bond respectively [Gu et al., 2019]. In the deconvoluted spectrum of O 1s (Figure 6.2 (d)), binding energies that appeared at 531.5, 532.3, and 533.5 eV are assigned for C=O, C-

O, and adsorbed oxygen respectively present in the material. Figure 6.2 (e) shows the core level spectrum of N 1s. Spectrum is deconvoluted into four prominent peaks present at 397.9, 398.5, 399.9, and 401.5 eV in which binding energy at 397.9 eV is ascribed to the cyanide group present in the PBA lattice, whereas component peaks at 398.5 and 399.9 eV are assigned with the pyridine N and graphitic N respectively. Oxide N corresponds to the binding energy at 401.5 eV [Zhou et al., 2018]. This further supports our synthesis of PBA nanocube along with FTIR. In addition, XPS analysis elucidates that the atomic ratio of Cu and Fe was found to be 3:2, which is in consistent with that of CuFe-PBA-NC precursor. Thus XPS analysis concludes the successful synthesis of PBA with its elements in their oxidation state along with the functional groups present in the molecule.

6.3.2. Oxidase activity of CuFe-PBA-NC and inhibition effect of INH

PBAs have found potential applications in the area of oxygen reduction and hydrogen evolution reaction with good catalytic properties. Also, Fe and Cu-based metal-organic frameworks have been reported as an excellent candidate for enzyme mimics [Nath et al., 2016]. Encouraged by these facts, the oxidase activity of the synthesized CuFe-PBA-NC was investigated.

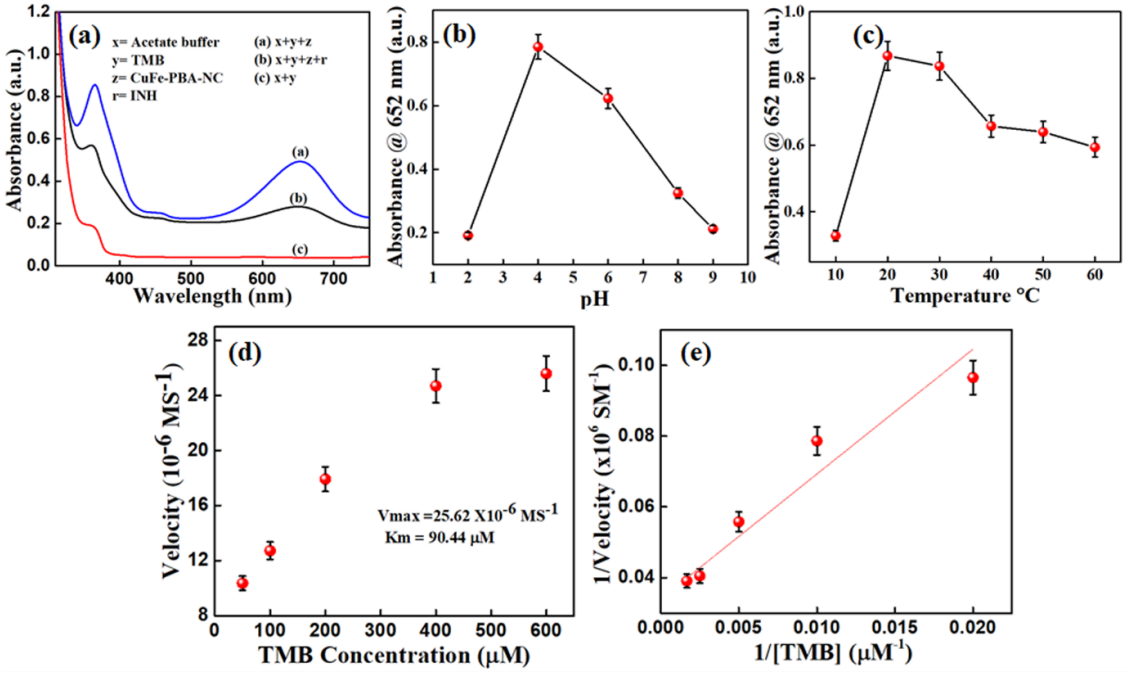

Figure 6.3. (a) Absorption spectra depicting the oxidase mimetic activity of the CuFe-PBA-NC and inhibition effect of INH (0.1M acetate buffer of pH=4; 100µL of 400µM TMB, CuFe-PBA-NC = 10µL (1mg/mL), 100 µL of 40µM INH). (b) Endpoint absorption spectra at λ_{max}=652 nm for optimization of pH, (c) Temperature. (d) Michaelis-Menten plot, and (e) Lineweaver Burk plot for TMB substrate in enzyme kinetic study.

In order to study the oxidase activity of the nanocube, the catalytic reaction was performed with chromogenic substrate TMB in the presence of dissolved oxygen. With the introduction of nanocube, TMB gets oxidized and displays its characteristic peaks at λ_{max} 370 and 652 nm in UV-Visible absorption spectra, as shown in Figure 6.3 (a). The peak corresponding to λ_{max} = 652 nm resulted from the charge transfer phenomenon between unoxidized and oxidized TMB, giving a characteristic blue charge transfer product. On the contrary, there is no oxidation of the TMB in the absence of nanocube, as shown in Figure 6.3. curve c. The oxidase activity of the CuFe-PBA-NC is inhibited in the presence of the INH and gives lower absorbance corresponding to the peak at λ_{max} = 652 nm (Figure 6.3a Curve b). The obtained result signifies the oxidase activity of the nanocube and the inhibition property of INH. The time-dependent study for the action

of INH on enzymatic reaction has been studied by recording the changes in absorbance value at λ_{max} = 652 nm with time, as shown in Figure 6.4.

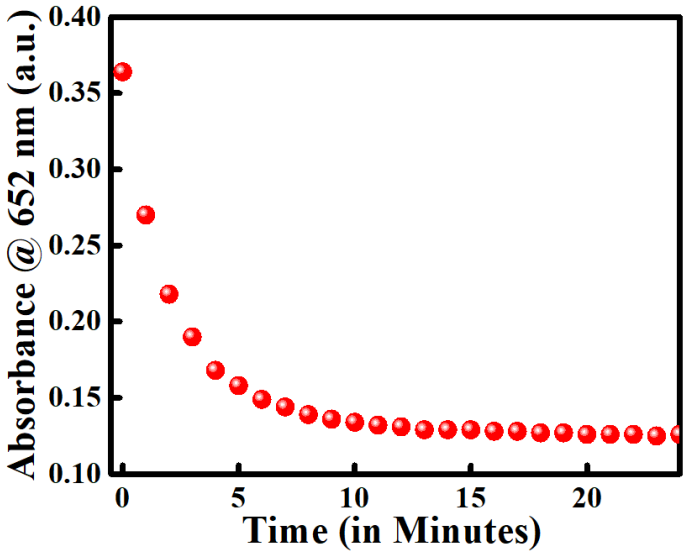

Figure 6.4. Time-dependent study of INH inhibition on oxidase activity of nanozyme.

It has been obtained that 20 minutes is required for the complete reaction of INH; therefore, for the colorimetric sensing, reaction mixtures were incubated for 20 minutes before recording the absorption spectrum.

6.3.3. Optimizations of pH and Temperature

The parameters like temperature and pH play a very significant role in the catalytic activity of the nanozymes. pH optimization has been done by varying the pH of the buffer solution. The endpoint absorption spectra were recorded at λ_{max}= 652 nm in five different buffer solutions of pH 2, 4, 6, 8, and 9. The colorimetric reaction was performed by adding 100 µL of buffers of different pH with 100µL of TMB (400mM) and 10µL of CuFe-PBA-NC (1mg/mL). It can be seen in Figure 6.3(b). that the oxidase activity of the nanozyme increases with pH from 2 to 4 and then decreases that is probably because diamine TMB has poor solutbilty at high pH [Ray et al., 2020]. The

result shows maximum absorbance at pH 4, depicting the optimum pH for the synthesized nanomaterial CuFe-PBA-NC which is also consistent with the work reported previously [Wei et al., 2008; Yang et al., 2017]. The enzyme activity of CuFe-PBA-NC has also been investigated at different temperatures (10, 20, 30, 40, 50, 60 ^{o}C). The reaction mixture was prepared by adding 100 μL of buffers of acetate of buffer pH with 100μL of TMB (400 mM) and 10μL of CuFe-PBA-NC (1mg/mL) and incubating it at different temperatures. Further, the endpoints have been recorded at λ_{max}= 652 nm, as can be observed in Figure 6.3(c). The nanozyme was found to be stable over a long range of temperatures and exhibits maximum activity in the range of 20 to 30 ^{o}C. The results show that CuFe-PBA-NC has better stability concerning pH and temperature than the natural enzyme HRP and has a wide range of temperatures to work. Further, all the experiments have been performed using the optimized conditions of temperature and pH.

6.3.4. Enzymes kinetics study

To investigate the kinetic of nanozyme, the experiments have been performed by taking different TMB concentrations (50, 100, 200, 400, 600 μM), keeping all other components invariable (i.e., acetate buffer and CuFe-PBA-NC). Figure 6.3 (d) shows the Michaelis-Menten plot where the endpoints at λ_{max}=652 nm were recorded with different concentrations of TMB substrate. Figure 6.3 (e) displays the Lineweaver-Burk Plot for TMB substrate. The obtained plots clearly signify that the synthesized nanozymes obey Michaelis-Menten kinetics which may be represented by the Michaelis-Menten equation given in Eq.6.1. In the equation, υ_0 represents initial velocity, [S] is the substrate concentration, V_{max} denotes maximum velocity, and K_m is

Michaelis–Menten constant (defined as substrate concentration (S) where the enzyme works with half of the maximum velocity).

$$\upsilon_0 = (V_{max}\,[S]) / (K_m + [S]) \qquad (6.1)$$

The enzyme velocity increases with the increase in the TMB concentration and reaches a saturation level where it becomes independent of substrate concentration. The optimized TMB concentration was found to be 400 μM. K_m and V_{max} value was calculated from the Lineweaver Burk plot, and their values were found to be 90.44 μM and 25.62×10^{-6} MS^{-1} respectively. The nanonzyme shows a lesser K_m value and greater V_{max} compared to HRP for the oxidation of TMB. The results show the better binding affinity of nanozymes towards chromogenic substrates with substantial catalytic efficiency because of the high surface area that allows more molecular interaction [Baldim et al., 2018; Sharma et al., 2015].

Table 6.1: Comparison table for the catalytic property of different nanozymes and HRP.

S.No.	Catalyst	Substrate	Km (mM)	Vmax	References
1	MoS_2	TMB	0.525	5.16×10^{-8}	Lin et al., 2014
2	C-dots	TMB	0.039	3.61×10^{-8}	Shi et al., 2011
3	HRP	TMB	0.434	10×10^{-8}	Chen et al., 2014
4	Si - Dots	TMB	1.502	14.72×10^{-8}	Chen et al., 2014
5	**CuFe-PBA-NC**	**TMB**	**0.09**	**2.6×10^{-5}**	**This work**

Table 6.1 shows the comparative study for K_m and V_{max} with respect to HRP and our nanozyme. It can be concluded that the nanozyme has better catalytic property and stability over the natural enzyme, HRP. A plausible mechanism for the colorimetric sensing of the INH using CuFe-PBA-NC has been proposed in the schematic (Scheme.6.1). The nanocube has been synthesized using a simple precipitation method, adding potassium ferricyanide into the sodium citrate and copper chloride solution in stirring condition at 760 rpm for 20 minutes. Furthermore, the reaction mixture was incubated for two days at RT. The synthesized nanomaterials show robust oxidase activity towards the chromogenic substrate TMB. The oxidation process of TMB has been well studied and confirmed by optical and EPR spectroscopy by Joseph et.al. [Joseph et.al., 1982]. Nanozyme acting as oxidase plays a role of catalyst which accelerates the oxidation reaction by mediating the electron transfer between TMB and dissolved oxygen well studied by Wenjie Qin. et al. TMB gets adsorbed to the nanocube's surface and transfers the electron to the nanocube and gets itself oxidized while adsorbed O_2 receives the electron and gets reduced [Quin et al., 2014]. TMB is colorless in its reduced form with λ_{max}=285 nm. However, in the presence of dissolved oxygen and nanocube, a cation-free radical is generated. Further, the oxidized TMB forms a charge-transfer complex with unoxidized TMB giving absorbance peaks at λ_{max}= 370 and 652 nm, which are responsible for the blue color observed during the oxidation of TMB. As per a report published by Shao-bin He et al. INH has a pyridine ring with a strong reductive hydrazyl group that provides the electron for reducing oxygen in place of TMB [He et al., 2020]. Therefore, INH shows competitive inhibitor property to the TMB molecules towards oxidase nanozyme. The INH introduction into the reaction mixture of TMB and CuFe-PBA-NC consequences a less efficient and colorless product in the oxidation of TMB. As the concentration of the INH increases,

the blue color of the product fades and gives blue color contrast with different concentrations of INH. Based on this inhibition concept, we have developed a colorimetric strategy for the quantification of the INH.

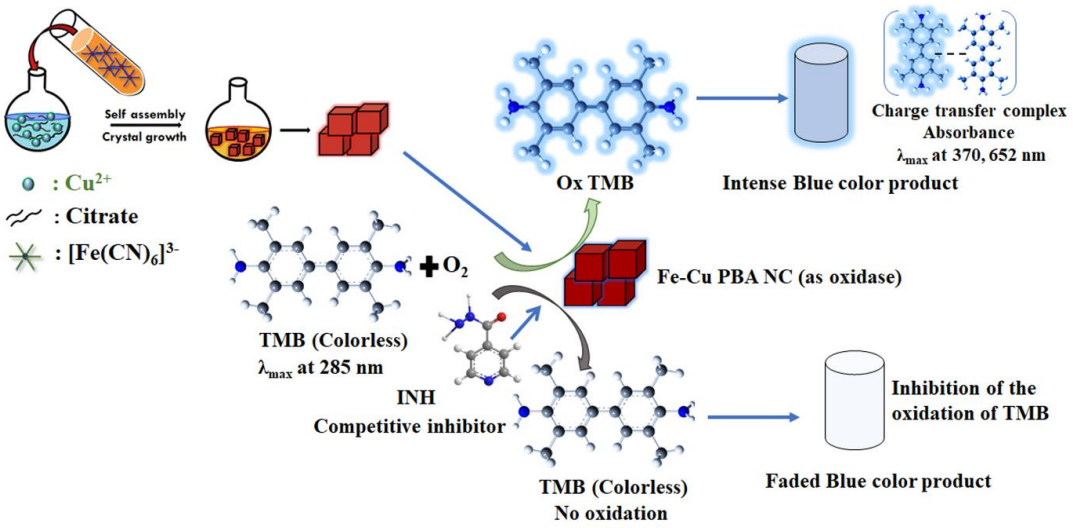

Scheme 6.1. Schematic showing the reaction principle for the oxidase activity of the CuFe-PBA-NC and colorimetric sensing of INH.

6.3.5. Colorimetric sensing of INH

The INH sensing has been done by exploiting its competitive inhibition property. On the addition of INH, the oxidase activity of the nanozyme is adversely affected, which results in color contrasts with different concentrations of the INH. For colorimetric sensing, seven different concentration of INH has been prepared by spiking the INH in acetate buffer (1, 10, 20, 30, 50, 75, 100 μM). Fig 6.5(a) shows the UV-Visible absorption spectra with an exponential decrease in the absorbance value at λ_{max} =370 and 652 nm with the increase in INH concentration (1 to 100 μM). The INH inhibitory effect of INH can be comfortably visualized with the naked eye as visible in the inset of Figure 6.5(a). Figure 6.5 (b) displays a calibration plot for INH and plotted by taking the average of the ten experiments performed in similar conditions. The inset Fig 6.5 (b) shows the linear response studied using the fitted-regression equation, where

absorbance at λ_{max} (652 nm) = 0.46007-0.00479 ×INH Conc. (μM) (R^2 =0.99) in the dynamic range of 1-50 μM. The developed sensors were found to be having a limit of detection (LOD) of 0.44 μM and were calculated using the ratio between three times standard deviations of the y-axis and the regression slope (LOD = (3*S_d)/slope).

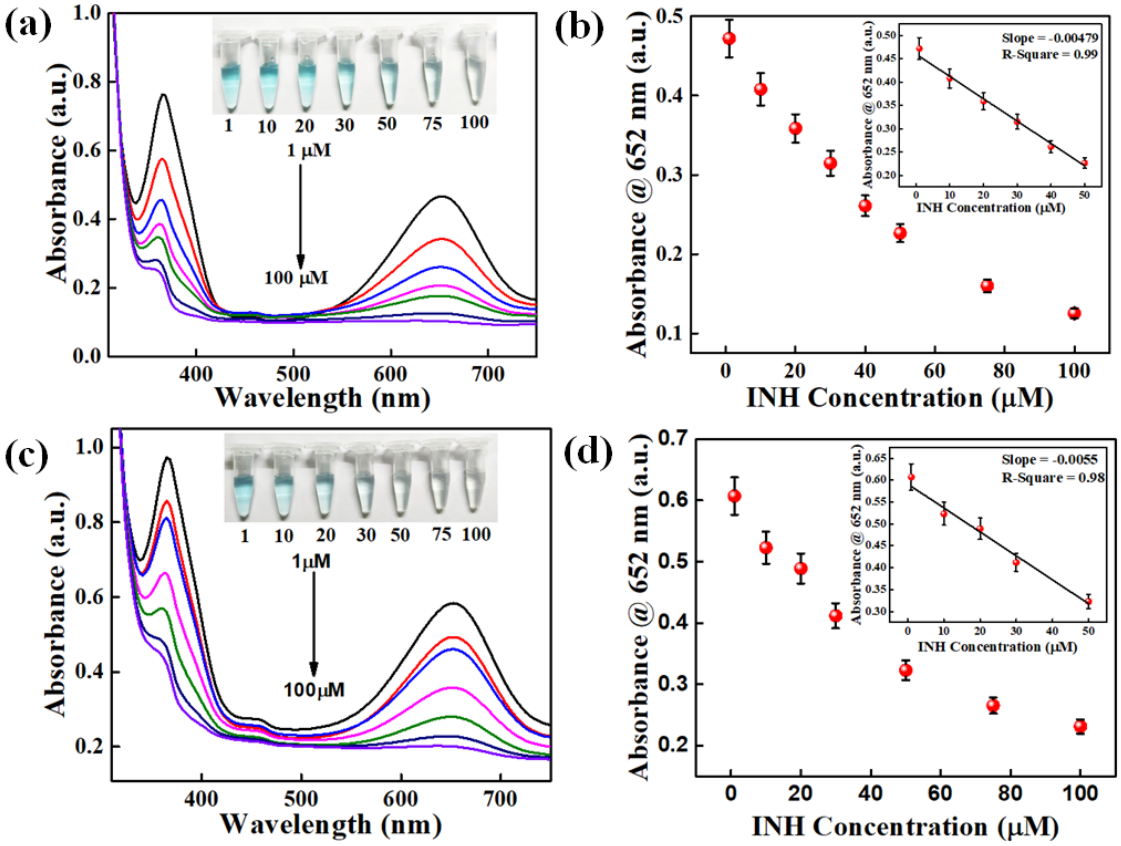

Figure 6.5 (a) Absorption spectra corresponding to different concentration of INH (1, 10, 20, 30, 50, 75, 100 μM) in 0.1 M acetate buffer (pH=4) with 400μM TMB and 1mg/mL CuFe-PBA-NC, (b) corresponding calibration plot of INH in 0.1M acetate buffer (pH= 4). Absorption spectra for the different INH concentrations in the human urine (1, 10, 20, 30, 50, 75, 100 μM), (d) calibration plot in human urine.

6.3.6. Real sample analysis

The activity of the nanozyme has also been used for the testing of the INH in the urine sample obtained from humans. Human urine samples have been incubated at 70 ^{o}C for 30 mins and centrifuged at 8000 rpm for 0.5 hours. Thus obtained filtrate was further filtered using a Nylon syringe filter with the pore diameter of 0.25 μM. The urine

sample was then diluted ten times with the acetate buffer of pH 4 and spiked with different concentrations of the INH (1, 10, 20, 30, 50, 75, 100 μM). As shown in Figure 6.5(c), the absorption spectrum was recorded using the same procedure optimized for the acetate buffer. The absorption spectra display a significant decrease of absorbance at λ_{max} =652 nm with the increase in INH concentration. Inset Figure 6.5(c) shows the color image pattern corresponding to different concentrations of INH. The calibration plot was studied using the fitted regression equation, the optical intensity at λ_{max} (652 nm) = 0.59111- 0.0055 ×INH Conc. (μM) (R^2 =0.98) in the dynamic range of 1-50 μM as shown in the inset of Fig 6.5 (d). The developed sensor shows an exponential decrease in the intensity with INH concentration with regression coefficient of 0.98, and the limit of detection was found to be 0.77 μM calculated using the ratio between three times standard deviations of the y-axis and the regression slope (LOD = (3*S_d)/slope).

6.3.7. Validation and Recovery study

The proposed colorimetric method was further validated using High-performance liquid chromatography (HPLC) by assessing the precision and accuracy of INH. The linearity of the validation assay was determined by measuring the response of five standard INH concentrations ranging from 10 to 160 μM. The HPLC chromatograms corresponding to 10, 20, 40, 80, and 160 μM are shown in Figures 6.6–6.13.

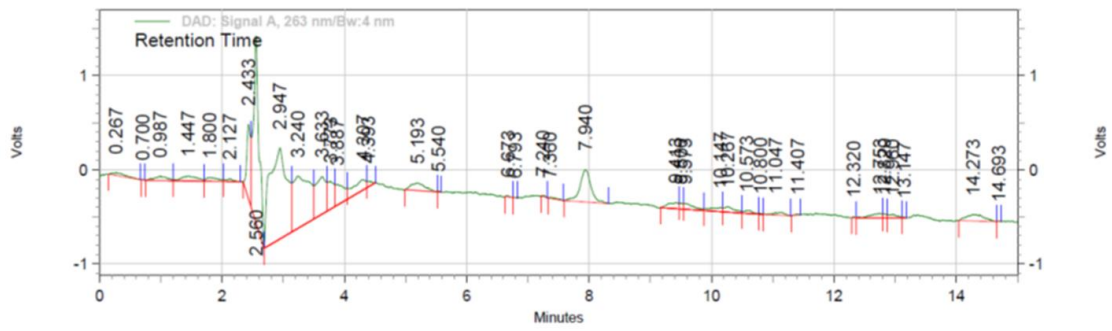

Figure 6.6. HPLC chromatogram in urine without INH.

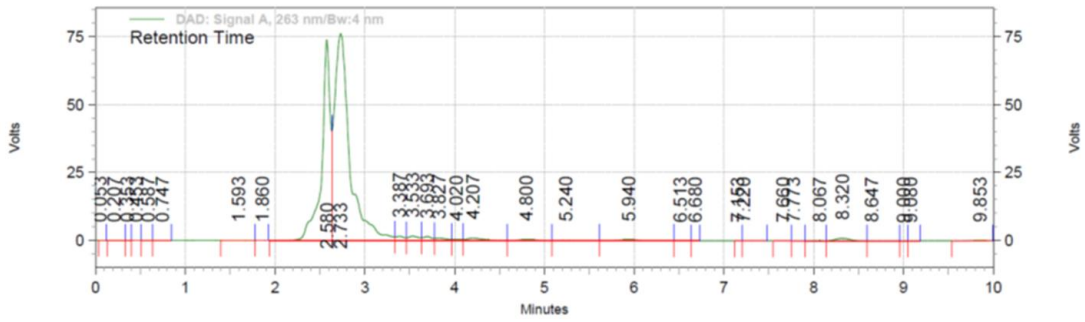

Figure 6.7. HPLC chromatogram urine with 10 μM INH.

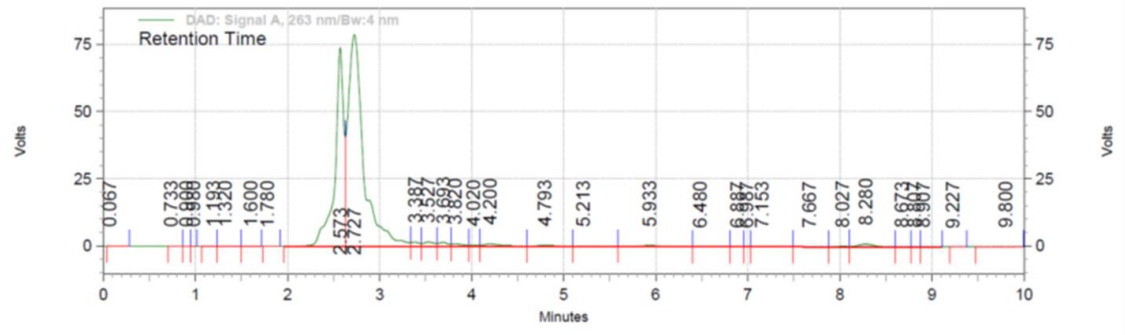

Figure 6.8. HPLC chromatogram in urine with 20 μM INH.

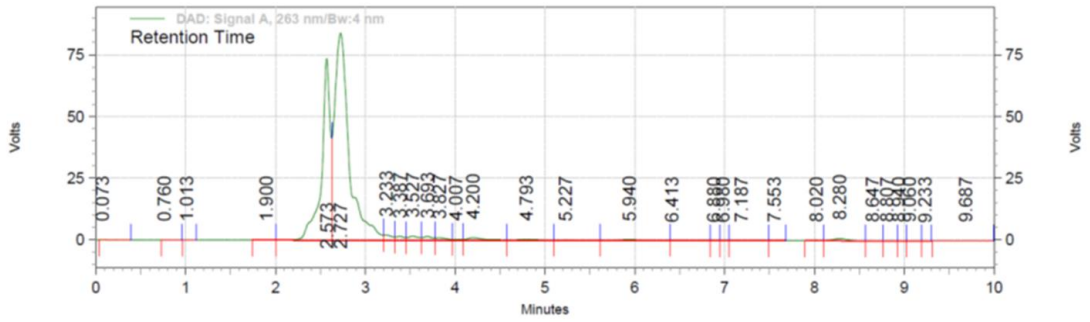

Figure 6.9. HPLC chromatogram in urine with 40 μM INH.

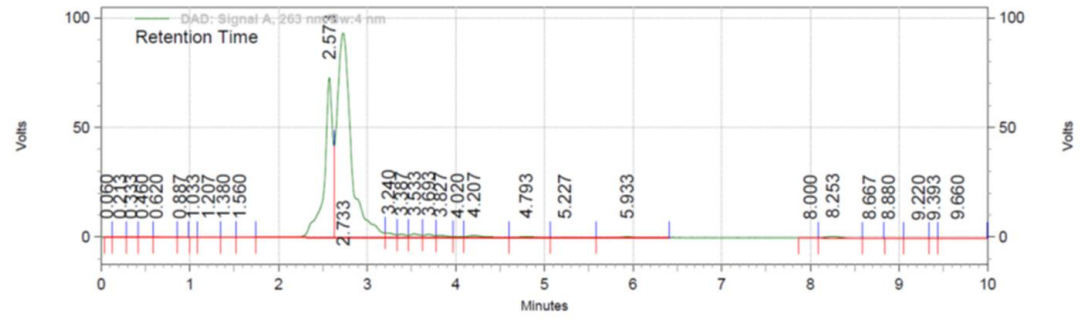

Figure 6.10. HPLC chromatogram in urine with 80 μM INH.

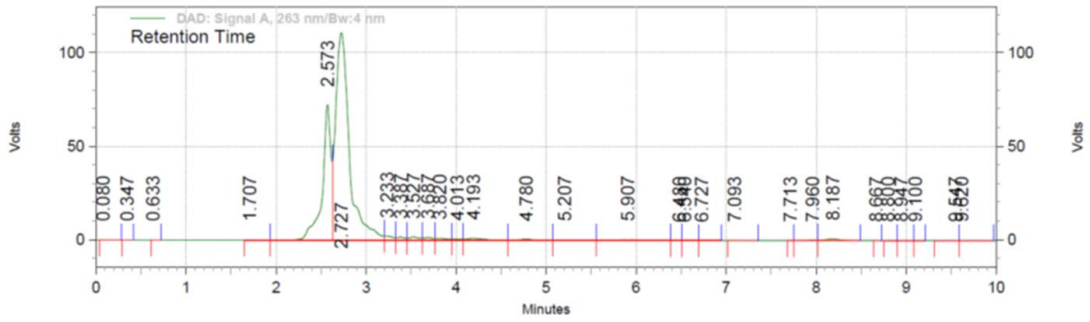

Figure 6.11. HPLC chromatogram in urine with 160 μM INH.

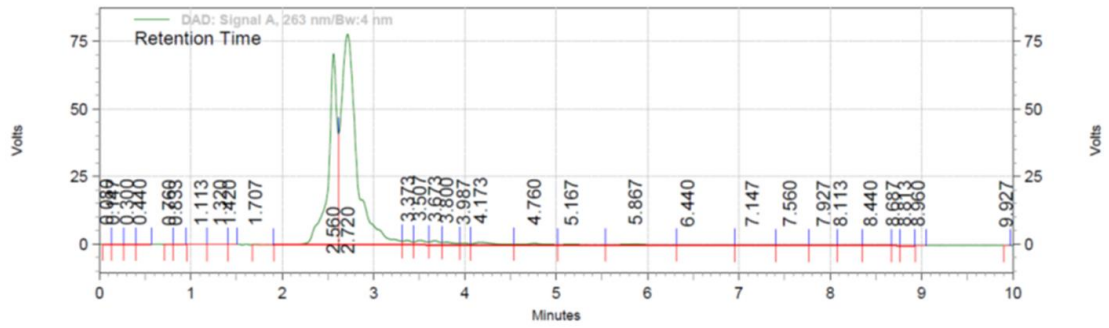

Figure 6.12. HPLC chromatogram for spiked sample A (15 μM INH).

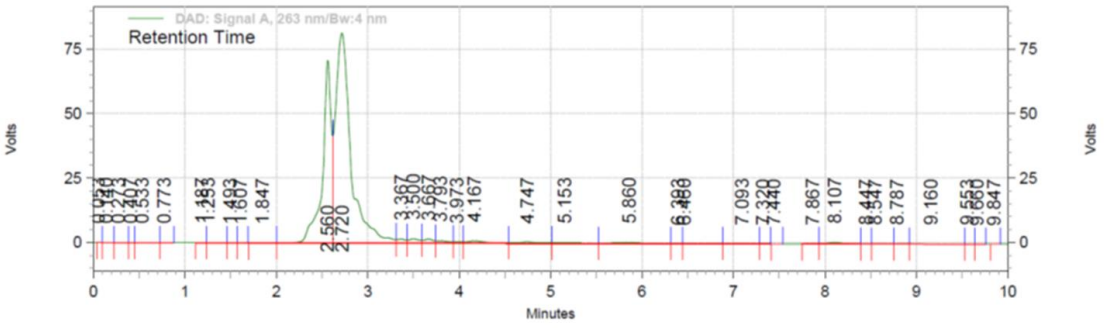

Figure 6.13. HPLC chromatogram for spiked sample B (30 μM INH).

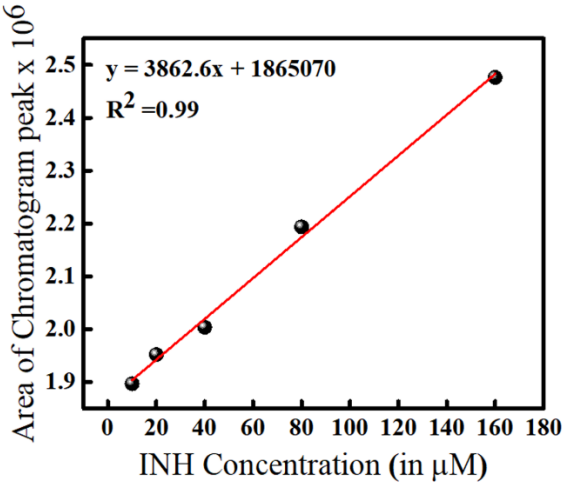

Figure 6.14. A linear relationship between the concentration of INH and the Area of the chromatogram obtained from the HPLC method.

The calibration plot was drawn showing the correlation between the peak area and concentration (Figure 6.14). The two spiked concentrations in urine samples 15 and 30

μM were used to study the precision and accuracy of the method. The concentration of the spiked samples was calculated using linear regression equation y = 3862.6×x + 1865070 (R^2=0.99), where y = area of chromatogram peak of INH corresponding to two spiked samples and x = concentration of spiked samples to be determined. The concentrations of spiked samples were also evaluated by our proposed colorimetric method. The comparative results were given in the recovery table and expressed as % recovery (Table 6.2), which validates good precision and accuracy of the proposed method over the selected concentrations.

Table 6.2: Recovery study of the urine samples.

Technique	**INH added (in μM)**	**INH found (in μM)**	**Recovery (%)**
HPLC	15	15.17	101.1
HPLC	30	31.7	105.7
This work (colorimetric)	15	14.6	97.3
This work (colorimetric)	30	32.5	108.3

6.3.8. Reproducibility

To test the consistency of the proposed method, the experiments were performed eight times in a similar set of conditions. In each test, six different concentrations (1, 10, 25, 50, 75, 100 μM) of INH were tested on the same day at an interval of an hour (intraday) and on four different days (interday). Figure 6.15 (a) and (b) show endpoint absorption spectra recorded at λ_{max} = 652 nm for the different concentrations of INH on the same

day (intraday) and on different days (interday), respectively. The result shows good consistency and reproducibility of the proposed method based on oxidase activity of the nanozyme.

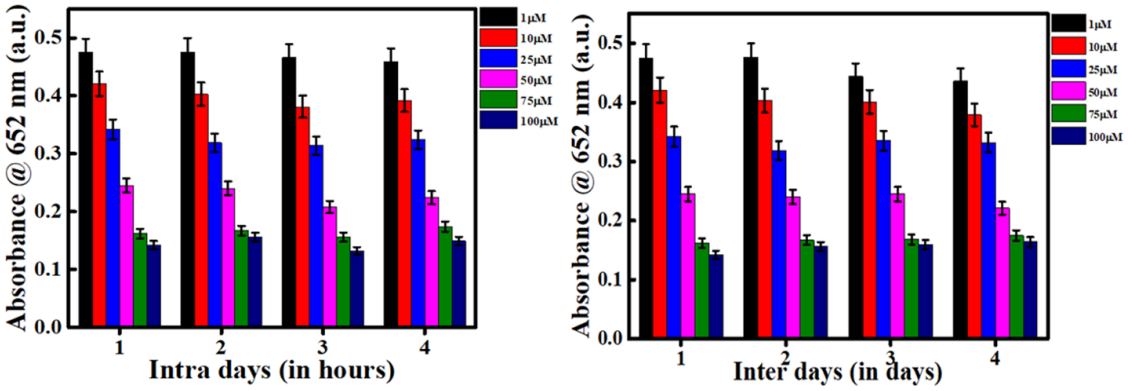

Figure 6.15. Reproducibility study. Endpoint absorption spectra at λ_{max}=652 nm of enzyme mimic in 0.1 M acetate buffer (pH=4) for the colorimetric reaction of TMB (400μM) with CuFe-PBA-NC in presence of INH (1,10, 25, 50, 75, 100 μM). (a) Intra study, and (b) Inter day study.

6.3.9. Interference study

The selectivity of the sensor for the INH has been investigated with the interferences present in the urine sample like Na^+, Cl^-, K^+, Glu, urea, Mg^{2+}, UA, and Creat. In order to elucidate the selectivity of the proposed sensor, the colorimetric reactions of TMB with CuFe-PBA-NC were performed in the presence of interferences and INH. The concentrations of the interferences have been taken ten-fold greater than the concentration of the INH for the testing. Figure 6.16 (a) shows the absorption spectrum depicting the effect of different analytes over the oxidase activity for the TMB oxidation. A bar diagram, as shown in Figure 6.16 (b), is given corresponding to the relative change of absorbance at λ_{max} =652 nm ($\Delta A = A_{blank}-A_{analyte}$) with different interferences and INH. The results clearly indicate good selectivity of the developed sensor for INH, showing a larger inhibition effect even at ten-fold lower concentration over the interferences. The obtained result and performance of the developed method

have been compared with the results of the previously reported methods on INH. As can be seen in Table 6.3, our work clearly shows the significance of nanocube as oxidase, giving better LOD, long linear range, and having good reproducibility. The proposed method gives economical sensing of INH and requires no sophisticated instrumentations. The synthesized nanocube also has the advantage of easy one-step synthesis and room temperature stability for its storage.

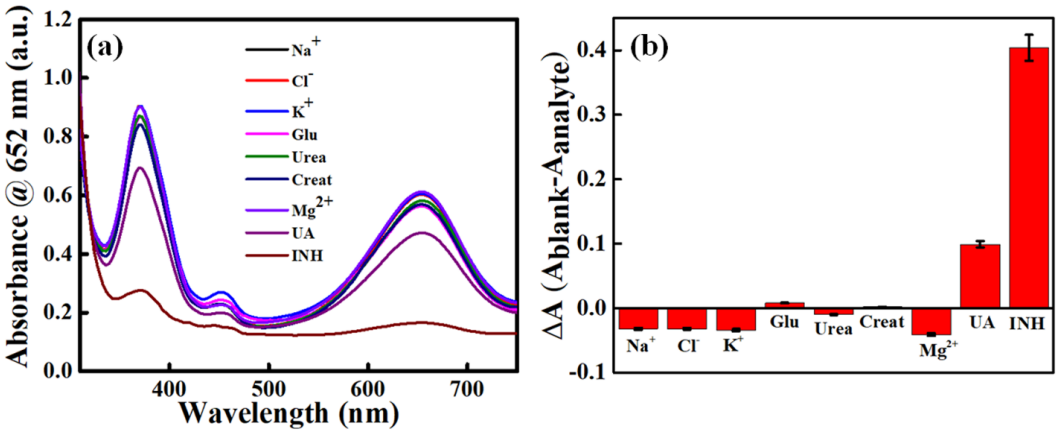

Figure 6.16. (a) UV-Visible absorption spectrum for interference study using colorimetric reaction of TMB (400 μM) with INH 100 μM and interferences 1000 μM in 0.1 M acetate buffer (pH=4) (b) Bar diagram showing the relative effect of the interferences with CuFe-PBA-NC oxidase and TMB colorimetric reaction in INH sensing.

Table 6.3. Comparison table for INH detection of some previous works and our method.

Nanomaterial	Techniques	Linear range (µM)	LOD (µM)	Buffer (pH)	Samples	References
Mxene	Voltammetry	100 to 4600	64	PBS (7.4)	Tablet, serum	Zhang et al., 2019
Rhodium	Linear sweep Voltammetry	70 to 1300	13	PBS (7)	Human urine, Blood plasma	Cheemalapati et al., 2014
Electrodeposited graphene and cysteic acid composite (CA/EGR)	Cyclic voltammetry	0.1 to 200	0.03	PBS (3.5)	Tablet, Serum	Majidi et al., 2006
Ag clusters on MnO_2 nano sheets	Fluorescent	0.8 to 200	0.47	HEPES (7.2)	Human urine, Serum	Liu et al., 2011
Au nanoparticles	Spectrophoto metric (LSPR)	1 to 8	0.98	PBS (8)	Tablet	Zargar et al., 2013
Fluorescence carbon dots (FCDs)	Fluorimetry	4 to 140	1.15	BR (4)	Tablet	Qin et al., 2019
Nitrogen-doped carbon dots (N-CDs) and MnO_2	Colorimetry and fluorimetry	2 to 120	0.7	Tris- HCl (7)	Tablet, serum	Ma et al., 2021
Functionalized MWCNTs and ZnO	Differential pulse voltammetry	2 to 28	0.012	PBS (5)	Tablet	Chokkareddy et al., 2020
Composite of MWCNTs and TiO_2NPs	Differential pulse voltammetry	0.5 to 5	0.03	PBS (7)	Tablet	Chokkareddy et al., 2017
CuFe-PBA-NC	**Colorimetry**	**1 to 50**	**0.44**	**Acetate buffer (4)**	**Human urine**	**This work**

6.3.10. Portable Eppendorf kit for INH detection

For the onsite detection of the INH, we have made a portable Eppendorf kit that can help in naked-eye detection (Figure 6.17). The device was developed using cheap Eppendorf through easy steps. 2 ml agarose suspension (20 mg/mL) was taken and boiled for 10 mins, followed by adding 100 μL of CuFe-PBA-NC and TMB (100 μL, 1mM), and a homogenous solution was obtained. The suspension was cooled to RT, and 100 μL was transferred to a cap of 0.5 mL Eppendorf and kept in the refrigerator for gel formation. For testing the sample containing INH, 100 μL of test samples with different INH concentrations (0-100 μM) were added to Eppendorf and kept inverted for 1 hour (Figure 6.17a). Figure 6.17b shows the response of the kit to different concentrations of INH in the urine sample (0, 1, 10, 20, 40, 50, 75, 100 μM). We have prepared a color scale with different blue color shades based on blue color contrast observed with an increase in the INH concentration in the Eppendorf kit (Figure 6.17c). This color scale may aid in the onsite detection of the INH.

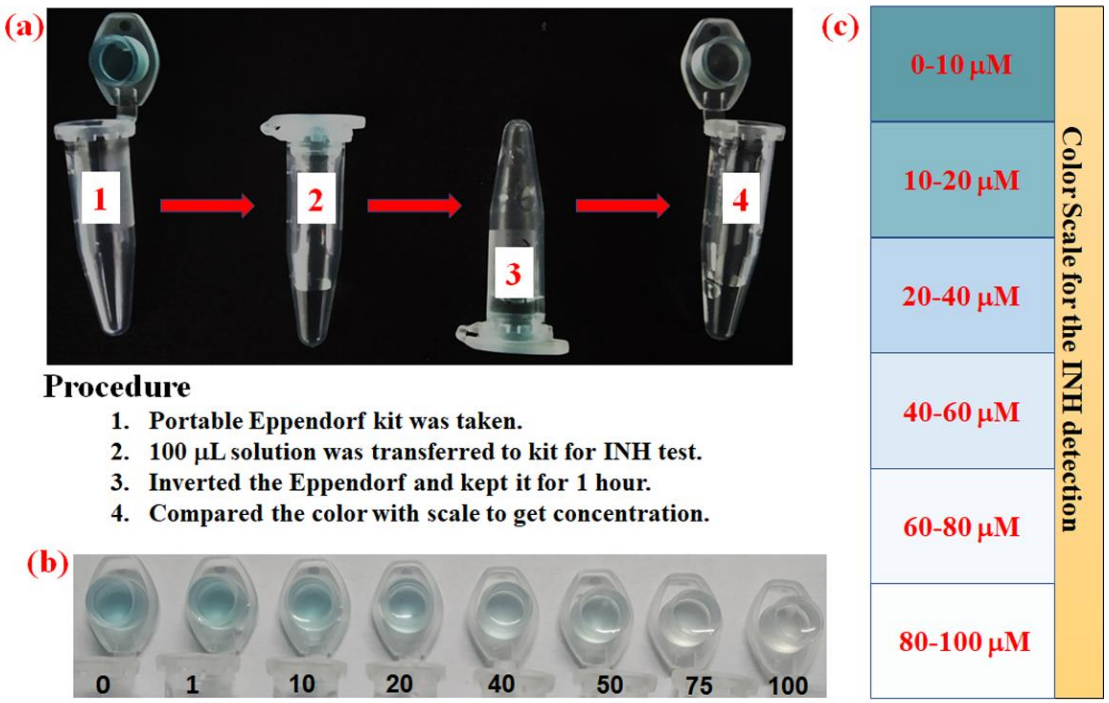

Figure 6.17. Portable Eppendorf kit-based detection of INH. (a) Procedure for the use of the kit. (b) Image showing kit response to different concentrations of INH. (c) The developed color scale for INH detection.

6.4. CONCLUSION

In conclusion, we have demonstrated the successful synthesis of CuFe-PBA-NC using a simple precipitation method and well-characterized by different techniques like IR, XRD, SEM, and XPS. The nanocubes of average size between 400-500 nm was found to be possessing high oxidase activity to TMB. We have efficiently utilized CuFe-PBA-NC to develop a selective and sensitive colorimetric strategy for sensing the anti-tuberculosis drug INH. The developed colorimetric sensor shows a wide range detection of INH in both acetate buffer and urine sample (1-100 µM) with LOD of 0.44 µM, 0.77 µM, respectively. We have also developed a portable Eppendorf kit which can be very helpful in the naked eye ultra-trace level onsite detection of INH. This technique shows a rapid, simple, and economical procedure with trace-level selective detection of INH in the human urine.